Integrated Remote Sensing Approaches for Predicting Sugarcane Yield in Fragmented Agricultural Lands

Cahyono, B. E.,[1*] Hakim, F. L.,[2] Indarto, I.[2] and Kurnianto, F. A.[3]
[1]Department of Physics, Universitas Jember, Jalan Kalimantan No. 37, Sumbersari, 68121, Jember, East Java, Indonesia, E-mail: bowo_ec.fmipa@unej.ac.id,* ORCID ID: https://orcid.org/0009-0007-5988-8744
[2]Department of Agricultural Engineering, Universitas Jember, 68121, Jember, East Java, Indonesia
E-mail: lukmanhakimfarid@gmail.com, ORCID ID: https://orcid.org/0000-0002-9669-7767,
indarto.ftp@unej.ac.id, ORCID ID: https://orcid.org/0000-0001-6319-6731
[3]Department of Geography Education, Universitas Jember, 68121, Jember, East Java, Indonesia
E-mail: fahmiarif.fkip@unej.ac.id, ORCID ID: https://orcid.org/0000-0002-3916-8930
Corresponding Author

DOI: https://doi.org/10.52939/ijg.v21i11.4595

Abstract
Sugarcane is a key raw material for sugar production and plays a significant role in Indonesia's economy. Efficient monitoring and yield estimation are therefore crucial, yet remain challenging due to geographic variation and climatic conditions. Previous studies on sugarcane yield estimation using satellite data have been largely conducted in extensive, homogeneous plantations. However, little attention has been given to fragmented smallholder sugarcane fields, where historical yield data are scarce and land management is heterogeneous. This study addresses this gap by developing and validating an estimation model using Sentinel-2 derived vegetation indices in smallholder sugarcane fields in East Java, Indonesia. Utilising Sentinel-2 satellite imagery, various vegetation indices—NDVI, GNDVI, NDII, NDRE, and SAVI—were employed as predictors. Data were collected from 38 sugarcane fields across four sub-districts and analysed in relation to actual yields. The results show that the maximum values of the vegetation indices exhibit a strong correlation with sugarcane yield, with NDVI having the highest correlation coefficient (r = 0.72). A multiple linear regression model revealed that index combinations provided the best accuracy: NDVI + GNDVI (R^2 = 0.65, RMSE = 11.32 t/ha), NDVI + NDII + NDRE (R^2 = 0.67, RMSE = 11.36 t/ha), and NDVI + NDII + SAVI (R^2 = 0.68, RMSE = 11.36 t/ha). These findings highlight the applicability of remote sensing-based approaches for yield prediction in fragmented smallholder systems, particularly sugarcane, offering a practical pathway to improve forecasting and support farm-level decision-making.

Keywords: Estimation, Regression, Sentinel-2, Vegetation Indices, Yield

1. Introduction

Agricultural sector plays a crucial role in Indonesia's economy, with sugar being one of the key commodities developed. Sugarcane industry and plantations have been integral to Indonesia's economic history for centuries, from colonial times to the modern era [1] and [2]. In the early 1930s, Indonesia reached a peak annual sugar production of nearly 3.0 million tons from 179 sugar factories, exporting 2.2 million tons to Europe [3]. Based on data from FAO [4], sugarcane production has shown an upward trend from 2010 to 2022. In 2022, Indonesia also ranked 27th as the largest exporter of sugar and its derivatives, valued at US$315 million, while simultaneously ranked third as the largest sugar importer, valued at US$1.79 billion [5].

East Java, one of Indonesia's largest provinces, plays a pivotal role in national sugar production. In 2022, it recorded the country's largest sugarcane cultivation area, covering 209,578 hectares and producing 1.2 million tons. Around 87% of this area is managed by smallholder farmers (Perkebunan Rakyat), while State-Owned Plantations and Private Plantations manage 12% and 1%, respectively. During 2018–2022, East Java's average annual sugar production reached 1.05 million tons, contributing 47.34% to national output [6][7] and [8]. This dominance highlights the importance of East Java as a focal region for national sugarcane studies.

However, despite its leading role, yield estimation and monitoring in the province remain challenging, particularly due to fragmented smallholder management systems. Despite Indonesia's vast potential in sugar production, challenges remain, especially in efficiently monitoring sugarcane crops and yield management. The country's geographic and climatic diversity complicates the monitoring and management of sugarcane plantations [9]. Field conditions, particularly in East Java, also reveal that many smallholder sugarcane farms are fragmented, and interspersed with other crops, such as paddy, corn, and other secondary crops, commonly referred to as *palawija* in Indonesia. Therefore, field-level studies on sugarcane yield estimation are crucial in addressing these constraints.

Utilisation of optical satellite imagery has become a valuable method for sugarcane yield estimation in many studies [10]. With its ability to provide a broad overview of agricultural land conditions, satellite imagery is an effective tool for monitoring sugarcane growth and development, especially on a regional/broad scale. The increasing availability of medium-resolution optical satellite imagery, such as Sentinel-2 and Landsat 8-9, has also greatly supported various spatial analysis studies [11] and [12]. Among these applications, the datasets have been particularly beneficial in enhancing agricultural land management and optimisation [13]. Sentinel-2 satellite using Multispectral Imager (MSI) sensor provides imagery with spatial resolution up to 10 meters and covers 13 spectral bands. Meanwhile, Landsat 8-9 using the Operational Land Imager (OLI) offers imagery with spatial resolution up to 30 meters and covers 9 spectral bands. These satellites are specifically designed and operated for continuous Earth surface monitoring missions [14]. This offers broad analysis possibilities, including land-use change monitoring, natural resource management, agricultural monitoring, and other types of analyses [15]. One widely developed application is the calculation of vegetation indices for monitoring agricultural land conditions.

Vegetation indices (VIs) are typically calculated using combinations of spectral bands from satellite imagery. They provide valuable information, including plant health, productivity, vigour, and density, by measuring plant reflectance across different wavelengths [16] and [17]. Researchers around the world have widely used VIs for numerous tasks such as crop monitoring, area mapping and calculation, evapotranspiration estimation, drought identification, and many other studies [18][19][20][21][22] and [23]. Many researchers also have utilised various VIs to predict agricultural yields, with the most commonly applied being the NDVI (Normalized Difference Vegetation Index) [24]. Researchers have also utilised other indices, including combining multiple indices to obtain accurate models [25] and [26].

Numerous studies have demonstrated the effectiveness of sugarcane yield estimation using VIs. NDVI derived from Moderate Resolution Imaging Spectroradiometer (MODIS), when integrated with artificial neural networks, has demonstrated the capability to estimate sugarcane yield in São Paulo, Brazil, anticipating the yield estimates by three months prior to harvest [27]. Furthermore, a comparative analysis of VIs extracted from Sentinel-2 imagery, conducted to predict sugarcane yield in Northern Karnataka, India, found that GNDVI achieved the strongest correlation with yield [28]. Additionally, another study in the Thakanto district, Thailand, underscored the importance of integrating multiple spectral information sources using Sentinel-2 and Landsat-8/9 datasets to improve sugarcane yield prediction accuracy [29]. Many other studies also show the capability of VIs to estimate yields for various agricultural/plantation commodities [30] and [31].

One of the estimation approaches use historical yield data as the primary input, known as the empirical approach [15]. However, significant constraints exist in collecting such historical data, particularly in smallholder plantations in East Java, where historical yield data is often poorly recorded or undocumented [32]. Another challenge is the widespread land lease system [33] and [34], which complicates the collection and tracking of farmers yield data, making it disorganised and difficult to manage. Furthermore, most agricultural land in East Java is fragmented into small, non-homogeneous plots due to land conversion and inheritance systems that have occurred for generations [35] and [36], which further adds to the challenges in developing accurate prediction models.

Therefore, this preliminary study is intended to develop a linear regression-based yield prediction model for Indonesia's fragmented and non-homogeneous agricultural land. This research aims to produce a yield prediction method based on farmer-reported yields, using various VIs as predictors across diverse land conditions and constraints. Through more comprehensive data processing, this research also aims to provide practical solutions for smallholder sugarcane farmers to optimise harvest planning and improve resource management.

2. Material and Methods

In this study, the methodological workflow (Figure 1) was designed to integrate field-based yield observations with Sentinel-2–derived predictors.

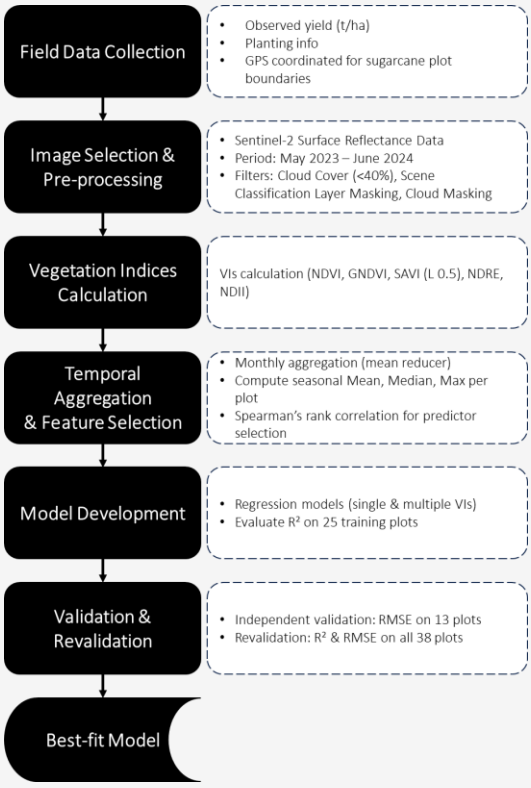

Figure 1: Workflow illustrating the development and validation of the sugarcane yield estimation model in fragmented smallholder fields using multi-temporal Sentinel-2 vegetation indices

The process began with field data collection from smallholder sugarcane plots, followed by satellite image preprocessing and vegetation indices calculation. These indices were then temporally aggregated to represent crop growth dynamics and statistically evaluated for their correlation with yield. The most relevant predictors were used to develop regression-based models, which were subsequently validated using independent field datasets. The workflow summarises this sequential approach from data acquisition to model validation, as detailed in Sections 2.1 to 2.4.

2.1 Study Area Overview

Four subdistricts Gumukmas, Umbulsari, Kencong, and Jombang were selected as the study locations, because it's the centres of sugarcane cultivation in Jember Regency, where sugarcane is the dominant crop. Geographically, Jember is situated in the eastern part of Java Island, Indonesia, covering an area of 3,306.7 km². The elevation in this region ranges from 0 to 3,096 meters above sea level and is flanked by two major volcanoes, Mount Argopuro and Raung [37]. Across Jember, the rainy season typically begins in October-November and lasts until April, with a total duration ranging from 18.1 to 19.1 ten-day periods. The Oldeman climate classification varies from C3 (5-6 wet months) in most areas to D3 (3-4 wet months) in the northwestern part, and E (<3 wet month) in the southern part, reflecting moderate to dry climatic conditions across the region [38] and [39]. The topography is predominantly flat in the central region along its main rivers, Bedadung and Mayang, while it becomes hilly in the southeastern/downstream areas. This region is also recognised as a prominent agricultural and plantation area in East Java Province, with key commodities including rice, tobacco, cocoa, coffee, rubber, and sugarcane [40].

2.2 Field Data Collection

Sugarcane yield data were collected from 38 smallholder farmers across four sub-districts: Gumukmas, Umbulsari, Kencong, and Jombang. These areas are located in the southern part of Jember Regency, where the planting season typically begins between June and August. The predominant sugarcane variety grown in these areas is *Bululawang* (BL), Indonesia's most widely cultivated variety, with an average harvest time of about 10-12 months, depending on its ripening type (early, mid, and late ripening), with yield up to 150 tons/ha [41][42] [43] and [44]. All sugarcane plots in this study follow the traditional *Sistem Juring Tunggal* (single-stool system), in which one sugarcane set is planted per hole with uniform spacing (row-to-row distance 70–100 cm; plant-to-plant distance 50–70 cm). Planting was conducted between June and August 2023 across all plots, resulting in slightly different crop ages at harvest. This uniform planting pattern, combined with known planting dates, ensures consistent canopy development and is relevant for spectral measurements and vegetation index calculations. The final yield data from each sugarcane plot were collected through farmer interviews during field visits between June 17 and September 17, 2024. Reported yields were based on field-scale records such as sales receipts or transport notes maintained by farmers, ensuring that the estimates reflected actual harvest outputs rather than farmer recall alone. These visits also gathered information about land ownership, planted varieties, and planting dates. Additionally, the geographic coordinates of each sugarcane plot were collected using SW Maps version 2.10.1.0, a free mobile GIS and mapping application [45]. The locations and summary statistics of the sugarcane plots are presented in Figure 2 and Table 1. The total plots were randomly divided into 25 plots (65%) for model training data, with the remaining 13 plots (35%) used for validation data.

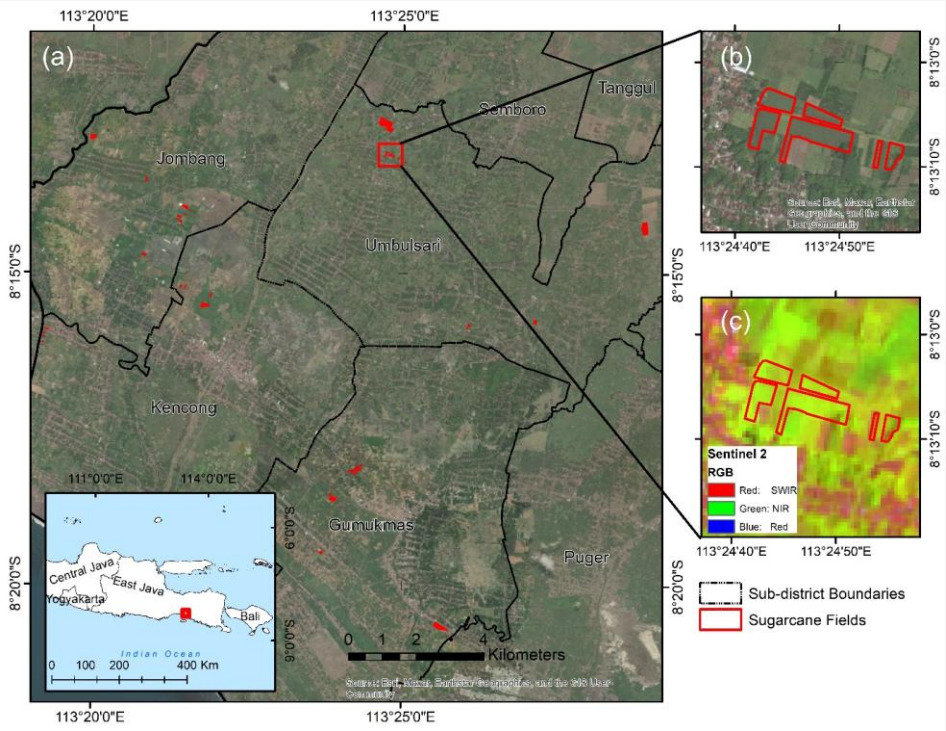

Figure 2: Spatial distribution of fragmented smallholder sugarcane fields in Jember Regency, East Java, Indonesia (a) locations of 38 sugarcane fields; (b) enlarged true colour composite; and (c) Sentinel-2 false-colour composite (SWIR, NIR, Red) of representative fields

Table 1: Summary statistics of the area and yield data from 38 sugarcane field plots

	Min	Max	Mean	Median	Std dev
Area (Ha)	0.10	7.69	1.26	0.67	1.68
Yield (Ton/Ha)	101.96	173.40	127.70	127.28	14.16

2.3 Satellite Data Collection and Processing

Sentinel-2 imagery was processed using the Google Earth Engine (GEE) platform. The images were acquired between May 2023 and June 2024, aligning with the sugarcane growing season in the study area. Sentinel-2 Level 2 (Surface Reflectance) images were used as the dataset, with two filters applied, cloud cover (<40%) and sugarcane plot boundary. A cloud masking script was also applied to reduce interference from cloud cover, which is prevalent in tropical regions and often poses challenges for optical imagery [46]. Additionally, the Scene Classification Layer available with Sentinel-2 data was utilised as a custom filter to retain only pixels previously classified as bare soil and vegetation, enhancing the quality of the imagery [47] and [48].

The selection process yielded 101 image scenes over the filtered period. The five vegetation indices were calculated from these selected images, as shown in Table 2. Within each plot, pixel-level VI values were first aggregated per month using the mean reducer in GEE to handle missing or cloud-affected pixels, typically resulting in 4–6 valid observations per month. Various studies indicate that the median reducer is the most commonly applied method for creating image composites; however, this study found that this method produced lower accuracy (results not shown), prompting us to opt for the mean reducer [49][50] and [51]. From these monthly averages, seasonal statistics including the mean, median, and maximum were computed for each plot.

In this study, linear regression and multiple linear regression were used as approaches to identify the best simple model for predicting sugarcane yields in fragmented land conditions and at relatively different phenological stages. Model fit was evaluated using the coefficient of determination (R^2) from the training dataset (25 plots), while predictive accuracy was assessed using the Root Mean Square Error (RMSE) on the independent validation dataset (13 plots). In addition, the selected model was revalidated on all 38 plots to provide overall performance metrics and spatially consistent yield predictions.

Table 2: Vegetation indices used in this study

Vegetation indices	Equation	Reference
Normalized Difference Vegetation Index (NDVI)	$NDVI = \frac{NIR - RED}{NIR + RED}$	[52]
Soil Adjusted Vegetation Index (SAVI)	$SAVI = \frac{NIR - RED}{(NIR + RED + L)(1 + L)}$	[53]
Green Normalized Difference Vegetation Index (GNDVI)	$GNVI = \frac{NIR - GREEN}{NIR + GREEN}$	[54]
Normalized Difference Red Edge (NDRE)	$NDRE = \frac{NIR - RED\ Edge}{NIR + RED\ Edge}$	[55]
Normalized Difference Infrared Index (NDII)	$NDII = \frac{NIR - SWIR}{NIR + SWIR}$	[56]

2.4 Vegetation Indices

This study used five vegetation indices NDVI, GNDVI, SAVI, NDRE, and NDII derived from Sentinel-2 imagery as predictors of sugarcane yield (Table 2). Vegetation index data were extracted throughout the entire growing season at a temporal resolution of five to ten days, in accordance with Sentinel-2's revisit cycle [57] and [58]. This high-frequency data acquisition enabled continuous monitoring of sugarcane growth dynamics and facilitated the identification of critical developmental stages. To determine the most effective predictor, an initial statistical analysis was conducted on the maximum (Max), mean (Mean), and median (Med) values of each index. These values were analysed for correlation with actual yield data to evaluate which metric provided the most accurate prediction. Spearman's Rank analysis was used to evaluate the relationship/correlation between vegetation indices and yield, allowing for the identification of non-linear trends that may not be detected by Pearson correlation [59].

3. Results and Discussion

An initial analysis was conducted on each index's maximum, mean, and median values, as shown in Table 3 below. Despite the application of a strict cloud-filtering threshold (<40%), temporal inconsistencies due to frequent cloud cover in tropical regions remain an inherent limitation when using optical satellite imagery. To mitigate these effects, we employed a temporal aggregation strategy by averaging vegetation index (VI) values at a monthly scale across the growing season. From these aggregated values, the maximum (Max), mean (Mean), and median (Med) VI were then derived to capture the variability of crop vigour stages. This approach not only minimises residual noise and potential outliers caused by cloud contamination, but also enhances the biological relevance of the predictor variables, as sugarcane yield is closely associated with the period of maximum canopy development. The maximum VI (Max) generally exhibits a more robust correlation compared to the mean (Mean) and median (Med). This indicates that the peak growth values of sugarcane have a greater influence on yield [60] and [61]. Based on the NDVI pattern depicted in Figure 3 below, the peak VIs for sugarcane in this region typically reach in February 2024, two to three months before harvest [62].

Table 3: Correlation coefficients of each vegetation index with actual yield data

Index	Correlation Coefficient
$NDVI_{max}$	0.725
$GNDVI_{max}$	0.429
$NDII_{max}$	0.672
$NDRE_{max}$	0.678
$SAVI_{max}$	0.678
$NDVI_{med}$	0.386
$GNDVI_{med}$	0.336
$NDII_{med}$	0.328
$NDRE_{med}$	0.436
$SAVI_{med}$	0.436
$NDVI_{mean}$	0.376
$GNDVI_{mean}$	0.262
$NDII_{mean}$	0.371
$NDRE_{mean}$	0.469
$SAVI_{mean}$	0.470

As the most commonly used VI, NDVI strongly correlates with yield, which indicates that vegetation density and health correlate with sugarcane productivity [63]. In contrast, GNDVI and NDRE are more sensitive to chlorophyll content. The lower correlation compared to NDVI may indicate that other factors besides chlorophyll also play significant roles in determining sugarcane yields [64] and [65].

Meanwhile, SAVI, designed to reduce soil brightness's influence, also shows a strong correlation [66]. Based on these initial correlation results, the maximum values of each vegetation index were used as predictors or input data in the regression analysis. Table 4 below shows the combinations of various vegetation indices used to predict sugarcane yield productivity by examining two main parameters: the coefficient of determination (R^2) and Root Mean Square Error (RMSE). R^2 describes how much variability in sugarcane productivity data can be explained by the regression model using a combination of vegetation indices. R^2 values range from 0 to 1, with values closer to 1 indicating that the model better explains data variation. In this context, a higher R^2 value means the model is more effective at explaining sugarcane productivity variation based on its independent variables (vegetation indices). On the other hand, RMSE indicates the average prediction error of the model, with the same unit as the predicted variable, i.e., tons/ha. RMSE provides insight into how far the model's predicted values are from the actual values. The lower the RMSE value, the more accurate the predictions generated by the model [67] and [68].

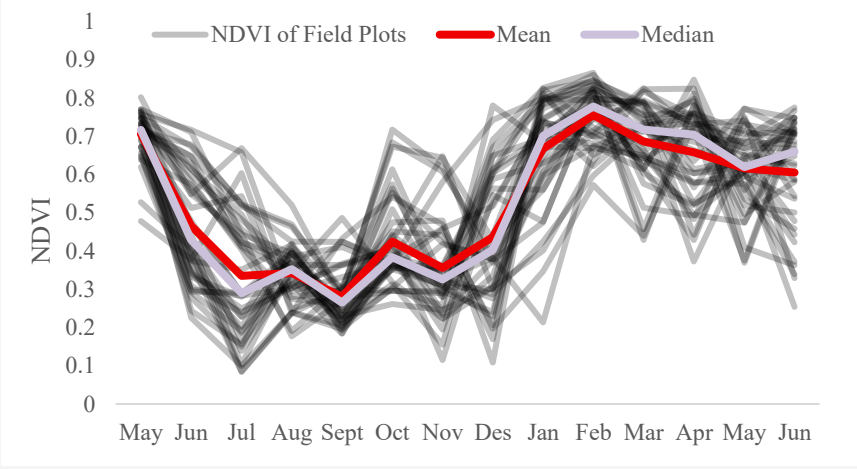

Figure 3: The variation of NDVI in relation to sugarcane growth

Table 4: The coefficient of determination and RMSE of each index and their combinations measured using validation plots. The numbers indicated in bold represent the best results

Index	ID	R^2	RMSE
NDVI	M1	0.525	11.522
GNDVI	M2	0.186	13.471
NDII	M3	0.452	11.892
NDRE	M4	0.460	11.980
SAVI	M5	0.460	11.980
NDVI + GNDVI	M6	0.653	**11.318**
NDVI + SAVI	M7	0.527	11.517
NDRE + SAVI	M8	0.468	12.061
NDVI + NDII + NDRE	M9	0.542	11.363
NDVI + NDII + SAVI	M10	0.542	11.363
GNDVI + NDRE + SAVI	M11	0.521	12.071
NDVI + GNDVI + NDRE + SAVI	M12	0.664	11.557
NDVI + NDII + NDRE + SAVI	M13	0.549	11.460
NDVI + GNDVI + NDII + SAVI	M14	0.655	11.412
NDVI + SAVI + NDII + GNDVI + NDRE	M15	**0.665**	11.637

Based on the validation results presented in the table, the combination of various vegetation indices shows significant differences in predicting sugarcane productivity. When using a single index, NDVI (M1) yields the best results with an R^2 of 0.525 and RMSE of 11.522, indicating that NDVI can explain approximately 52.54% of the variability in sugarcane productivity. Other indices, such as GNDVI (M2), have a significantly lower R^2 (0.1863) with an RMSE of 13.471, suggesting that this index alone does not provide accurate predictions. Meanwhile, other indices like NDII (M3), NDRE (M4), and SAVI (M5) offer moderate results but still fall below NDVI.

When two indices are combined, the predictions become more accurate, with the combination (M6) (NDVI + GNDVI) achieving the best R^2 and RMSE, respectively, of 0.653 and 11.318. This combination enhances the model's ability to explain sugarcane productivity variability to 65.28%, with lower prediction errors than single indices. Combinations of three indices, such as (M9) and (M10), show steady improvements with an R^2 of 0.542 and an RMSE of around 11.36, although not as high as the best two-index combination. In four to five index combinations, such as (M12) and (M15), while R^2 reaches 0.665, the increase in prediction accuracy does not accompany a significant reduction in RMSE. The six index combinations with the best RMSE results are then used to estimate yields across all plots and cross-validated with actual harvest results collected from farmers to assess the prediction model's accuracy on a larger sample. Figure 4 below shows the scatter plot from this revalidation.

Based on the revalidation using a scatterplot comparing sugarcane yield estimates with actual harvest data (Figure 4), it was found that the combination (M6) (NDVI + GNDVI) still provided the best results with a coefficient of determination (R^2) of 0.461 and an RMSE of 12.890. This indicates that this combination can explain about 46.09% of the variability in sugarcane yield, with a relatively low prediction error. This two-index combination proved the most effective in predicting yields among all tested combinations. NDVI is an excellent indicator for predicting sugarcane yield because it is closely related to two key yield components: biomass and sugar content. During the growth phase, NDVI closely correlates with the Leaf Area Index (LAI), which reflects the density and surface area of the plant's leaves [69] and [70]. LAI influences photosynthesis and biomass accumulation, indicating that a high NDVI value can represent optimal sugarcane growth [71]. Additionally, during the maturation and ripening phases, NDVI also reflects changes in leaf colour and canopy density, which are associated with aboveground biomass accumulation [72]. As sugarcane matures, the structural changes in the crop can significantly impact the total yield harvested [73][74][75] and [76].

Although NDVI is a widely used, many research found that it has certain limitations, particularly saturation issues at high biomass levels, which can reduce its sensitivity in dense crop canopies [77][78] and [79]. As an index that uses the green spectral band, GNDVI was found to reduce this saturation issue. The green band (0.560 nm) has greater penetration into leaf canopy [80], making it more effective for assessing vegetation vigour in high-density crops such as sugarcane [81] and [82]. Moreover, GNDVI is particularly sensitive to chlorophyll content and photosynthetic activity [83][84] and [85], which are critical factors in biomass accumulation and overall crop health.

NDVI and GNDVI combination provides stronger predictive performance probably due to their complementary strengths. NDVI effectively tracks biomass accumulation and sugar content changes, while GNDVI enhances sensitivity to chlorophyll variations and reduces saturation effects. This synergy leads to more accurate yield estimations, as shown by lower RMSE values and higher R^2 scores in predictive models. By integrating both indices, the model can capture a broader range of crop conditions, leading to improved precision in sugarcane yield predictions. The second-best combination is (M14), which yielded R^2 and RMSE values of 0.456 and 12.890, respectively. Although the R^2 value is slightly lower than that of combination (M6), adding other indices like NDII and SAVI enhanced the model's capacity to explain yield variability, but not enough to significantly reduce the RMSE value. Despite a slightly higher prediction error, this combination still provided satisfactory results.

NDII, which primarily indicates the water content in crops [85], has the potential to correlate with sugarcane yield, as water availability plays a crucial role in crop growth and productivity [86]. However, despite its relevance, the inclusion of NDII did not significantly improve the predictive accuracy in terms of reducing RMSE. Similarly, SAVI, which is designed to minimise the impact of soil brightness [87], has shown potential in improving the stability of spectral reflectance relationships with crop yield, particularly in areas with low vegetative cover. Another research have highlighted the advantages of distance-based vegetation indices like SAVI in refining NDVI-based yield predictions [88].

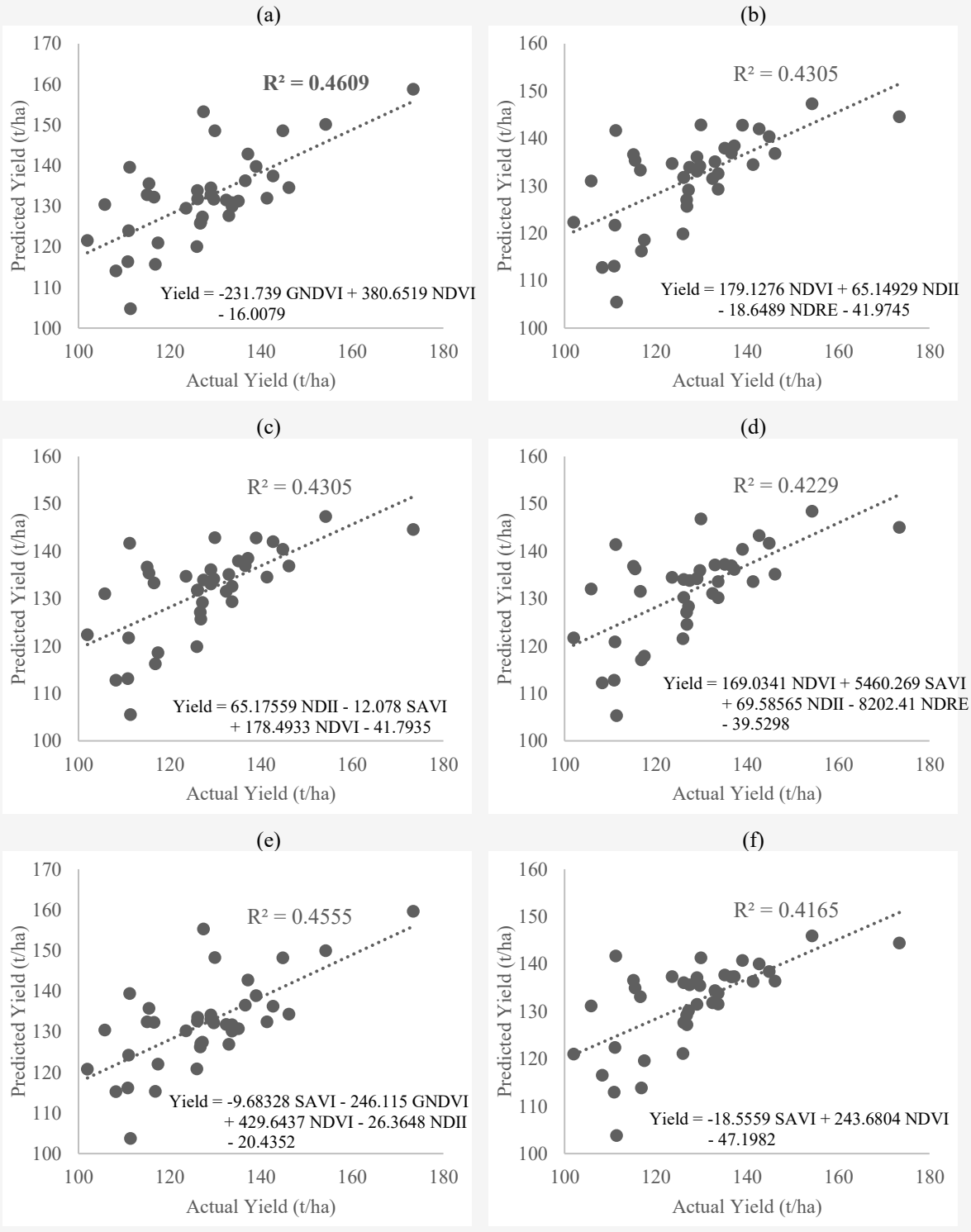

Figure 4: Sugarcane yield validation for the six highest RMSE values:
(a) M6, (b) M9, (c) M10, (d) M13, (e) M14, (f) M7

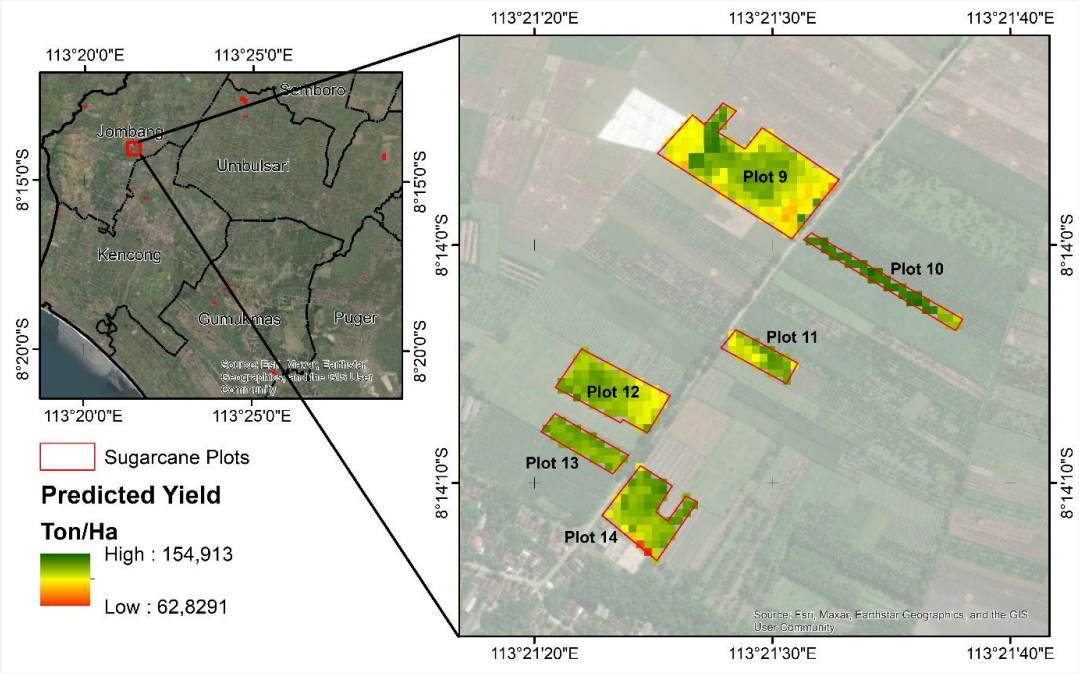

Figure 5: Spatial distribution of predicted sugarcane yield (t/ha) for six adjacent plots (Plots 9–14) within the study area, derived from the NDVI + GNDVI model

However, in this study, while SAVI contributed to explaining sugarcane yield variability, it did not substantially lower the prediction error. This suggests that while NDII and SAVI hold promise for improving yield estimation models, further refinement and additional datasets are needed to fully leverage their potential in sugarcane yield prediction. Overall, it can be concluded that while several combinations with three to four indices yielded promising results, the NDVI + GNDVI (M6) combination remains the most efficient, offering the best balance between the ability to explain yield variability (R^2) and achieving low prediction error (RMSE). In this study, more complex models, while enhancing explanatory capacity, did not always lead to significant reductions in prediction errors; therefore, more straightforward yet effective models are recommended. To further illustrate the applicability of this model at the field scale, a spatial analysis was conducted for six adjacent plots (Plots 9–14) within the study area (Figure 5). This figure demonstrates how the model operates at the pixel level and highlights yield variability both within and across fields, reflecting the fragmented nature of sugarcane cultivation in East Java.

The results revealed both consistencies and deviations. For instance, Plot 9 showed strong agreement between prediction (131.41 t/ha) and actual yield (133.66 t/ha), whereas Plot 10 was notably overestimated (142.78 vs. 126.11 t/ha) and Plot 13 was underestimated (134.61 vs. 146.13 t/ha). The remaining plots displayed moderate deviations, generally within 5–8 t/ha. These findings highlight that while the model effectively captures yield patterns, discrepancies can still arise at the field level, particularly where local management and soil conditions differ [10] and [89].

Such deviations are not uncommon in linear regression models, which assume uniform relationships across all fields. In contrast, machine learning (ML) approaches, such as Random Forests or Gradient Boosting, could potentially reduce these errors by capturing nonlinearities and site-specific interactions between vegetation indices and yield. While the present study focused on a parsimonious multiple linear regression for interpretability and practicality, future work could compare its performance against ML-based methods to determine whether prediction errors at the field scale can be minimised further.

4. Conclusion

This preliminary study explores the potential use of vegetation indices derived from Sentinel-2 satellite imagery to predict sugarcane yield in fragmented agricultural lands. This study has developed a new approach for estimating sugarcane yield production by evaluating the correlation of maximum values of single and multiple vegetation indices with actual yield data collected from farmers. The analysis shows that NDVI has the strongest correlation with sugarcane yield among the five indices tested,

followed by NDRE, SAVI, NDII, and GNDVI. Maximum vegetation index values are more effective than average and median values in estimating sugarcane productivity. Fifteen types of treatments, both single and combinations of several indices, were tested in this study. However, the combination of the two indices, NDVI + GNDVI, produced a more accurate predictive model with an R^2 value of 0.65 and a lower RMSE (11.318 ton/ha) than combinations of three to five indices.

Furthermore, the temporal aggregation strategy used to handle frequent cloud cover in tropical regions ensures that the vegetation indices reliably capture peak crop development, enhancing the robustness of the predictive model. Overall, this research successfully demonstrates that remote sensing technology based on satellite imagery can provide an efficient solution for monitoring and predicting sugarcane yield, particularly in fragmented and heterogeneous agricultural land such as Indonesia, using a linear regression approach.

Thus, the findings of this study can assist farmers and land managers in improving agricultural management efficiency through more accurate yield predictions. It is important to emphasise that this research should be further developed, especially by using machine learning-based regression approaches such as Random Forest, Support Vector Regression, and Artificial Neural Networks, as these methods have the potential to enhance model accuracy. Nevertheless, it should be noted that this study represents an initial step in developing a predictive model for sugarcane yield and is based on a limited dataset. The findings and model performance should be validated with a more extensive dataset covering different regions, soil conditions, and climatic variations to ensure robustness and generalisability.

Acknowledgements

Thank you to The Ministry of Research, Technology, and Higher Education of Republic Indonesia for the supporting research funding through the Fundamental Research Scheme in 2024.

References

[1] Heryanto, M. A. and Suryatmana, E. R., (2020). Dinamika Agroindustri Gula Indonesia: Tinjauan Analisis Sistem [Dynamics of Indonesia's Sugar Agroindustry: A Systems Analysis Review]. *Agricore: Jurnal Agribisnis Dan Sosial Ekonomi Pertanian Unpad*, Vol. 5(2), 194–210. https://doi.org/10.24198/agricore.v5i2.32100.

[2] Nawiyanto, N., Capili, J. W. and Calvaryni, N. M., (2023). The Colonial Sugar Industry in Indonesia and the Philippines: A Comparative Perspective. *Paramita: Historical Studies Journal*, Vol. 33(2), 244–254. https://doi.org/10.15294/paramita.v33i2.46347.

[3] Toharisman, A., Triantarti and Hasan, M. F., (2013). Rise and Fall of the Indonesian Sugar Industry. *International Society Sugar Cane Technology*, Vol. 28, 1992–1998.

[4] FAOSTAT - Crops and Livestock Products. *Food and Agriculture Organization of the United Nations*. [Online]. Available: https://www.fao.org/faostat/en/#data/QCL. [Accessed: Jun. 03, 2024]

[5] The Sweet Escape: Indonesia's Growing Obsession with Sugar. *The Jakarta Post*. [Online]. Available: https://www.thejakartapost.com/front-row/2022/05/27/the-sweet-escape-indonesias-growing-obsession-with-sugar.html. [Accessed: May 27, 2024].

[6] Respati, E., (2022). Outlook Komoditas Perkebunan Tebu [Outlook of the Sugarcane Plantation Commodity]. *Satu Data Pertanian*. [Online]. Available: https://satudata.pertanian.go.id/assets/docs/publikasi/Outlook_Tebu_2022.pdf. [Accessed: Mar. 7, 2024].

[7] BPS-Statistics Indonesia. (2022). Statistik Tebu Indonesia 2022 [Indonesia Sugar Cane Statistics 2022] (Direktorat Statistik Tanaman Pangan Hortikultura dan Perkebunan (ed.); Vol. 13. BPS-Statistics Indonesia.

[8] BPS-Statistics of Jawa Timur Province. (2023). Provinsi Jawa Timur dalam Angka 2023 [Jawa Timur Province in Figures 2023]. BPS-Statistics of Jawa Timur Province.

[9] Pramuhadi, G., (2016). *Faktor Iklim Pada Budidaya Tebu Lahan Kering [Climatic Factors in Dryland Sugarcane Cultivation]. Jurnal Pangan*, Vol. 19(4), 331–344.

[10] de França e Silva, N. R., Chaves, M. E. D., Luciano, A. C. dos S., Sanches, I. D., de Almeida, C. M. and Adami, M., (2024). Sugarcane Yield Estimation Using Satellite Remote Sensing Data in Empirical or Mechanistic Modeling: A Systematic Review. *Remote Sensing*, Vol. 16(5). https://doi.org/10.3390/rs16050863.

[11] Song, X. P., Huang, W., Hansen, M. C. and Potapov, P., (2021). An Evaluation of Landsat, Sentinel-2, Sentinel-1 and MODIS Data for Crop Type Mapping. *Science of Remote Sensing*, Vol. 3. https://doi.org/10.1016/j.srs.2021.100018.

[12] Trevisiol, F., Mandanici, E., Pagliarani, A. and Bitelli, G., (2024). Evaluation of Landsat-9 Interoperability with Sentinel-2 and Landsat-8 over Europe and Local Comparison with Field Surveys. *ISPRS Journal of Photogrammetry and Remote Sensing*, Vol. 210, 55–68. https://doi.org/10.1016/j.isprsjprs.2024.02.021.

[13] Segarra, J., Buchaillot, M. L., Araus, J. L. and Kefauver, S. C., (2020). Remote Sensing for Precision Agriculture: Sentinel-2 Improved Features and Applications. *Agronomy*, Vol. 10(5). https://doi.org/10.3390/agronomy10050641.

[14] Masek, J. G., Wulder, M. A., Markham, B., McCorkel, J., Crawford, C. J., Storey, J. and Jenstrom, D. T., (2020). Landsat 9: Empowering Open Science and Applications Through Continuity. *Remote Sensing of Environment*, Vol. 248. https://doi.org/10.1016/j.rse.2020.111968.

[15] Weiss, M., Jacob, F. and Duveiller, G., (2020). Remote Sensing for Agricultural Applications: A Meta-review. *Remote Sensing of Environment*, Vol. 236. https://doi.org/10.1016/j.rse.2019.111402.

[16] Xue, J. and Su, B. (2017). Significant Remote Sensing Vegetation Indices: A Review of Developments and Applications. *Journal of Sensors*, Vol. 2017(1), 1–17. https://doi.org/10.1155/2017/1353691.

[17] Ali, Z., Jaelani, L., and Sumargana, L. (2024). Detection of Corn Phenological Stages with Landsat Satellite Imagery: A Case Study in Ngawi Regency, Indonesia. *International Journal of Geoinformatics*, Vol. 20(9), 1–15. https://doi.org/10.52939/ijg.v20i9.3535.

[18] Zuhro, A., Tambunan, M. P. and Marko, K., (2020). Application of Vegetation Health Index (VHI) to Identify Distribution of Agricultural Drought in Indramayu Regency, West Java Province. *IOP Conference Series: Earth and Environmental Science*, Vol. 500(1). https://doi.org/10.1088/1755-1315/500/1/012047.

[19] Sari, N. M., Indra, T. L. and Kushardono, D., (2022). Urban Vegetation Quality Assessment Using Vegetation Index and Leaf Area Index from Spot 7 Data with Fuzzy Logic Algorithm. *International Journal on Advanced Science, Engineering and Information Technology*, Vol. 12(2). https://doi.org/10.18517/ijaseit.12.2.11719.

[20] Camps-Valls, G., Campos-Taberner, M., Moreno-Martínez, Á., Walther, S., Duveiller, G., Cescatti, A., Mahecha, M. D., Muñoz-Marí, J., García-Haro, F. J., Guanter, L., Jung, M., Gamon, J. A., Reichstein, M. and Running, S. W., (2021). A Unified Vegetation Index for Quantifying the Terrestrial Biosphere. *Science Advances*, Vol. 7(9), 1–10. https://doi.org/10.1126/sciadv.abc7447.

[21] Radhi, F., Khalil, S., and Ali, S. (2025). Drought Monitoring using Remote Sensing-Based Indices in the Southern Region of Iraq. *International Journal of Geoinformatics*, Vol. 21(6), 1–11. https://doi.org/10.52939/ijg.v21i6.4227.

[22] Olivares-Campos, B. O., Paredes, F., Rey, J. C., Lobo, D. and Galvis-Causil, S., (2021). The Relationship Between the Normalized Difference Vegetation Index, Rainfall, and Potential Evapotranspiration in a Banana Plantation of Venezuela. *SAINS TANAH - Journal of Soil Science and Agroclimatology*, Vol. 18(1). https://doi.org/10.20961/stjssa.v18i1.50379.

[23] Hidayati, I. N., Suharyadi, R. and Danoedoro, P., (2018). Exploring Spectral Index Band and Vegetation Indices for Estimating Vegetation Area. *Indonesian Journal of Geography*, Vol. 50(2). https://doi.org/10.22146/ijg.38981.

[24] Boonma, R., Suwanprasit, C., and Homhuan, S. (2024). Modeling Rice Growth and Yield using Integrated Remote Sensing Data on Google Earth Engine. *International Journal of Geoinformatics*, Vol. 20(11), 116–133. https://doi.org/10.52939/ijg.v20i11.3693.

[25] Karlson, M., Ostwald, M., Bayala, J., Bazié, H. R., Ouedraogo, A. S., Soro, B., Sanou, J. and Reese, H., (2020). The Potential of Sentinel-2 for Crop Production Estimation in a Smallholder Agroforestry Landscape, Burkina Faso. *Frontiers in Environmental Science*, Vol. 8, 1–13. https://doi.org/10.3389/fenvs.2020.00085.

[26] Tiruneh, G. A., Meshesha, D. T., Adgo, E., Tsunekawa, A., Haregeweyn, N., Fenta, A. A., Alemayehu, T. Y., Mulualem, T., Fekadu, G., Demissie, S. and Reichert, J. M., (2023). Mapping Crop Yield Spatial Variability using Sentinel-2 Vegetation Indices in Ethiopia. *Arabian Journal of Geosciences*, Vol. 16(11). https://doi.org/10.1007/s12517-023-11754-x.

[27] Fernandes, J. L., Francisco, N., Ebecken, F. and César, J., (2017). Sugarcane Yield Prediction in Brazil Using NDVI Time Series and Neural Networks Ensemble. *International Journal of Remote Sensing*, Vol. 38(16), 4631–4644. https://doi.org/10.1080/01431161.2017.1325531.

[28] Jha, S. K., Patil, V. C., Rekha, B., Virnodkar, S. S., Bartalev, S. A., Plotnikov, D., Elkina, E. and Patel, N., (2022). Sugarcane Yield Prediction Using Vegetation Indices in Northern Karnataka, India. *Universal Journal of Agricultural Research*, Vol. 10(6), 699–721. https://doi.org/10.13189/ujar.2022.100611.

[29] Som-ard, J., Suwanlee, S. R., Pinasu, D., Keawsomsee, S., Kasa, K., Seesanhao, N., Ninsawat, S., Borgogno-Mondino, E. and Sarvia, F., (2024). Evaluating Sugarcane Yield Estimation in Thailand Using Multi-Temporal Sentinel-2 and Landsat Data Together with Machine-Learning Algorithms. *Land*, Vol. 13. https://doi.org/https://doi.org/10.3390/land13091481.

[30] Perich, G., Turkoglu, M. O., Graf, L. V., Wegner, J. D., Aasen, H., Walter, A. and Liebisch, F., (2023). Pixel-based Yield Mapping and Prediction from Sentinel-2 using Spectral Indices and Neural Networks. *Field Crops Research*, Vol. 292. https://doi.org/10.1016/j.fcr.2023.108824.

[31] Ribeiro, A. L. A., Maciel, G. M., Siquieroli, A. C. S., Luz, J. M. Q., Gallis, R. B. de A., Assis, P. H. de S., Catão, H. C. R. M. and Yada, R. Y., (2023). Vegetation Indices for Predicting the Growth and Harvest Rate of Lettuce. *Agriculture*, Vol. 13(5). https://doi.org/10.3390/agriculture13051091.

[32] Rusdiyanto, Zulfauzi, and Zulius, A., (2019). Perancangan Timbangan Pencatat Hasil Panen Otomatis Menggunakan Mikrokontroler Berbasis Web Dan Database [Design of an Automatic Harvest Recording Scale Using a Web- and Database-Based Microcontroller]. *Jusikom: Jurnal Sistem Komputer Musirawas*, Vol. 04(02), 93–99.

[33] Utomo, S. J. and Wulandari, D., (2020). Sistem Sewa Lahan Pertanian Masyarakat Pedesaan dalam Perspektif Ekonomi [Agricultural Land Leasing Systems in Rural Communities from an Economic Perspective]. *JDEP (Jurnal Dinamika Ekonomi Pembangunan)*, Vol. 3(1), 27–33. https://doi.org/10.33005 /jdep.v3i1.101.

[34] Ambarwati, A., Kusuma, R. A., Pratama, Y. A. and Astuti, W. P., (2021). Sistem Maro pada Pengelolaan Lahan Pertanian Berkelanjutan di Desa Tlawong [The Maro System in Sustainable Agricultural Land Management in Tlawong Village]. *Solidarity: Journal of Education, Society and Culture*, Vol. 10(2), 117–126.

[35] Umyati, S., Andayani, S. A. and Ismannudin, I., (2022). Fragmentasi Lahan dan Tingkat Kesejahteraan Petani Bawang Merah: Sebuah Analisis Review [Land Fragmentation and the Welfare Level of Shallot Farmers: A Review Analysis]. *JSEP (Journal of Social and Agricultural Economics)*, Vol. 15(1). https://doi.org/10.19184/jsep.v15i1.29272.

[36] Mulyono, J. and Munibah, K. (2017). Strategi Pembangunan Pertanian di Kabupaten Bantul dengan Pendekatan A'WOT [Agricultural Development Strategy in Bantul Regency Using the A'WOT Approach]. *Jurnal Pengkajian Dan Pengembangan Teknologi Pertanian*, Vol. 19(3). https://doi.org/10.21082/jpptp.v19n3.2016.p199-211.

[37] National Aeronautics and Space Administration [NASA] JPL. (2013). NASA Shuttle Radar Topography Mission Global 1 arc second. [Data set]. NASA EOSDIS Land Processes DAAC. https://doi.org/10.5067/MEaSUREs/SRTM/SRTMGL1.003.

[38] Riajaya, P. D., (2020). Rainy Season Period and Climate Classification in Sugarcane Plantation Regions in Indonesia. *IOP Conference Series: Earth and Environmental Science*, Vol. 418(1). https://doi.org/10.1088/1755-1315/418/1/012058.

[39] Aldiansyah, S. and Risna, R., (2023). Mapping of Oldeman Agro-Climatic Zone Based on Climate Hazards Group Infrared Precipitation with Station Database in Southeast Sulawesi. *ECOTROPHIC: Jurnal Ilmu Lingkungan (Journal of Environmental Science)*, Vol. 17(2). https://doi.org/10.24843/EJES.2023.v17.i02.p02.

[40] Aunurrofiq, F., Sumarjono, Swastika, K., Na'im, M. and Surya, R. A., (2020). Afdeeling Djember: Bureaucratic History of Jember During the Dutch Colonial Era 1883-1928. *IOP Conference Series: Earth and Environmental Science*, Vol. 485(1). https://doi.org/10.1088/1755-1315/485/1/012142.

[41] Widyasari, W. B., Putra, L. K., Ranomahera, M. R. R. and Puspitasari, A. R., (2022). Historical Notes, Germplasm Development, and Molecular Approaches to Support Sugarcane Breeding Program in Indonesia. *Sugar Tech*, Vol. 24(1), 30–47. https://doi.org/10.1007/s12355-021-01069-0.

[42] Faesol, N., Avivi, S., Hariyono, K., Ubaidillah, M. and Hartatik, S., (2022). Yield Characteristics and Stability of Sugarcane Mutant in Three-Location Trials. *Universal Journal of Agricultural Research*, Vol. 10(6), 838–845. https://doi.org/10.13189/ujar.2022.100621.

[43] Yunita, R., Hartati, R. S., Suhesti, S. and Syafaruddin. (2020). Response of Bululawang Sugarcane Variety to Salt Stress. *IOP Conference Series: Earth and Environmental Science*, Vol. 418(1). https://doi.org/10.1088/1755-1315/418/1/012060.

[44] Sulaiman, A. A., Subagyono, K., Soetopo, D., Richana, N., Syukur, M., Hermanto, and Ardana, I. K., (2018). Menjaring Investasi Meraih Swasembada Gula [Mobilising Investment to Achieve Sugar Self-Sufficiency] (M. Sardjono & B. Marwoto (eds.); Edisi 1). IAARD PRESS.

[45] Aviyaan Tech. (2024). SW Maps (2.10.1.0). [Mobile Application]. Available: https://aviyaantech.com/swmaps/. [Accessed: Sept. 24, 2024].

[46] Indarto, I. and Hakim, F. L., (2021). Tracking Land Use Land Cover Changes from 2000 to 2018 in a Local Area of East Java Province, Indonesia. *Bulletin of Geography. Socio-Economic Series*, Vol. 52(52), 7–24. https://doi.org/10.2478/bog-2021-0010.

[47] Nowak, B., Marliac, G. and Michaud, A. (2021). Estimation of Winter Soil Cover by Vegetation Before Spring-sown Crops for Mainland France using Multispectral Satellite Imagery. *Environmental Research Letters*, Vol. 16(1). https://doi.org/https://doi.org/10.1088/1748-9326/ac007c.

[48] Sanchez, C., Mena, F., Charfuelan, M., Nuske, M. and Dengel, A., (2024). Assessment of Sentinel-2 Spatial and Temporal Coverage Based on The Scene Classification Layer. *In IGARSS 2024-2024 IEEE International Geoscience and Remote Sensing Symposium*, Vol. July, 4099–4103. https://doi.org/10.48550/arXiv.2406.18584.

[49] Chaulagain, S., Stone, M. C., Morrison, R. R., Yang, L., Coonrod, J. and Villa, N. E. (2023). Determining the Response of Riparian Vegetation and River Morphology to Drought Using Google Earth Engine and Machine Learning. *Journal of Arid Environments*, Vol. 219. https://doi.org/10.1016/j.jaridenv.2023.105068.

[50] Pu, D. C., Sun, J. Y., Ding, Q., Zheng, Q., Li, T. T. and Niu, X. F., (2020). Mapping Urban Areas using Dense Time Series of Landsat Images and Google Earth Engine. *The International Archives of the Photogrammetry, Remote Sensing and Spatial Information Sciences*, Vol. XLII-3/W10(3/W10, 403–409. https://doi.org/10.5194/isprs-archives-XLII-3-W10-403-2020.

[51] Phan, T. N., Kuch, V. and Lehnert, L. W., (2020). Land Cover Classification using Google Earth Engine and Random Forest Classifier—The Role of Image Composition. *Remote Sensing*, Vol. 12(15). https://doi.org/10.3390/rs12152411.

[52] Thammaboribal, P. (2024). Investigating Land Surface Temperature Variation and Land Use Land Cover Changes in Pathumthani, Thailand (1997-2023) using Landsat Satellite Imagery: A Comprehensive Analysis of LST and Urban Hot Spots (UHS). *International Journal of Geoinformatics*, Vol. 20(2), 27–41. https://doi.org/10.52939/ijg.v20i2.3063..

[53] Andita, A., and Hidayati, N. (2025). Assessing CO2 Absorption of Urban Trees Using NDVI, SAVI, and MSARVI in Salatiga, Indonesia. *International Journal of Geoinformatics*, Vol. 21(4), 18–34. https://doi.org/10.52939/ijg.v21i4.4063.

[54] Gitelson, A. A., Kaufman, Y. J. and Merzlyak, M. N., (1996). Use of a Green Channel in Remote Sensing of Global Vegetation from EOS-MODIS. *Remote Sensing of Environment*, Vol. 58(3), 289–298. https://doi.org/10.1016/S0034-4257(96)00072-7.

[55] Barnes, E. M., Clarke, T. R., Richards, S. E., Colaizzi, P. D., Haberland, J., Kostrzewski, M., Waller, P., Choi C., R. E., Thompson, T., Lascano, R. J., Li, H. and Moran, M. S., (2000). Coincident Detection of Crop Water Stress, Nitrogen Status and Canopy Density Using Ground Based Multispectral Data. *Proceeding of the 5th International Conference Precision Agriculture*. 1-15

[56] Fensholt, R. and Sandholt, I., (2003). Derivation of a Shortwave Infrared Water Stress Index from MODIS Near- and Shortwave Infrared Data in a Semiarid Environment. *Remote Sensing of Environment*, Vol. 87(1), 111–121. https://doi.org/10.1016/j.rse.2003.07.002.

[57] Li, J. and Chen, B., (2020). Global Revisit Interval Analysis of Landsat-8 -9 and Sentinel-2A -2B Data for Terrestrial Monitoring. *Sensors*, Vol. 20(22). https://doi.org/10.3390/s20226631.

[58] Sentinel-2 User Handbook. ESA Standard Document. *European Space Agency*. [Online]. Available: https://sentinel.esa.int/documents/247904/685211/Sentinel-2_User_Handbook. [Accessed: May 20, 2024].

[59] Bermudez-Edo, M., Barnaghi, P. and Moessner, K., (2018). Analysing Real World Data Streams with Spatio-Temporal Correlations: Entropy Vs. Pearson Correlation. *Automation in Construction*, Vol. 88, 87–100. https://doi.org/10.1016/j.autcon.2017.12.036.

[60] Dubrovin, K. N., Stepanov, A. S. and Aseeva, T. A., (2022). Application of LAI and NDVI to Model Soybean Yield in the Regions of the Russian Far East. *IOP Conference Series: Earth and Environmental Science*, Vol. 949(1). https://doi.org/10.1088/1755-1315/949/1/012030.

[61] Groten, S. M. E., (1993). NDVI Crop Monitoring and Early Yield Assessment of Burkina Faso. *International Journal of Remote Sensing*, Vol. 14(8), 1495–1515. https://doi.org/10.1080/01431169308953983.

[62] Bégué, A., Lebourgeois, V., Bappel, E., Todoroff, P., Pellegrino, A., Baillarin, F. and Siegmund, B., (2010). Spatio-Temporal Variability of Sugarcane Fields and Recommendations for Yield Forecast Using NDVI. *International Journal of Remote Sensing*, Vol. 31(20), 5391–5407. https://doi.org/10.1080/01431160903349057.

[63] Huang, J., Wang, H., Dai, Q. and Han, D., (2014). Analysis of NDVI Data for Crop Identification and Yield Estimation. *IEEE Journal of Selected Topics in Applied Earth Observations and Remote Sensing*, Vol. 7(11), 4374–4384. https://doi.org/10.1109/JSTARS.2014.2334332.

[64] Boiarskii, B. and Hasegawa, H., (2019). Comparison of NDVI and NDRE Indices to Detect Differences in Vegetation and Chlorophyll Content. *Journal of Mechanics of Continua and Mathematical Sciences*, Vol. 4, 20–29. https://doi.org/10.26782/jmcms.spl.4/2019.11.00003.

[65] Voitik, A., Kravchenko, V., Pushka, O., Kutkovetska, T., Shchur, T. and Kocira, S., (2023). Comparison of NDVI, NDRE, MSAVI and NDSI Indices for Early Diagnosis of Crop Problems. *Agricultural Engineering*, Vol. 27(1), 47–57. https://doi.org/10.2478/agriceng-2023-0004.

[66] Care, F. R. A. M., Subagio, B. S. and Rahman, H. (2018). Porous Concrete Basic Property Criteria as Rigid Pavement Base Layer in Indonesia. *MATEC Web of Conferences*, Vol 147. https://doi.org/10.1051/matecconf/201814702008.

[67] Akossou, A. Y. J. and Palm, R., (2013). Impact of Data Structure on the Estimators R-Square and Adjusted R-Square in Linear Regression. *International Journal of Mathematics and Computation*, Vol. 20(3), 84–93.

[68] Hodson, T. O., (2022). Root-Mean-Square Error (RMSE) or Mean Absolute Error (MAE): When to Use Them or Not. *Geoscientific Model Development*, Vol. 15(14), 5481–5487. https://doi.org/10.5194/gmd-15-5481-2022.

[69] Carlson, T. N. and Ripley, D. A., (1997). On the Relation Between NDVI, Fractional Vegetation Cover, and Leaf Area Index. *Remote Sensing of Environment*, Vol. 62(3), 241–252. https://doi.org/10.1016/S0034-4257(97)00104-1.

[70] Pérez, G., Coma, J., Chàfer, M. and Cabeza, L. F., (2022). Seasonal Influence of Leaf Area Index (LAI) on the Energy Performance of a Green Facade. *Building and Environment*, Vol. 207. https://doi.org/10.1016/j.buildenv.2021.108497.

[71] de Oliveira Maia, F. C., Bufon, V. B. and Leão, T. P., (2023). Vegetation Indices as a Tool for Mapping Sugarcane Management Zones. *Precision Agriculture*, Vol. 24(1), 213–234. https://doi.org/10.1007/s11119-022-09939-7.

[72] Wani, A. A., Bhat, A. F., Gatoo, A. A., Zahoor, S., Mehraj, B., Najam, N., Wani, Q. S., Islam, M. A., Murtaza, S., Dervash, M. A. and Joshi, P. K., (2021). Assessing Relationship of Forest Biophysical Factors with NDVI for Carbon Management in Key Coniferous Strata of Temperate Himalayas. *Mitigation and Adaptation Strategies for Global Change*, Vol. 26(1). https://doi.org/10.1007/s11027-021-09937-6.

[73] Simões, M. dos S., Rocha, J. V. and Lamparelli, R. A. C., (2005). Growth Indices and Productivity in Sugarcane. *Scientia Agricola*, Vol. 62(1), 23–30. https://doi.org/10.1590/S0103-90162005000100005.

[74] Leandro, E. R., Heenkenda, M. K. and Romero, K. F., (2024). Estimating Sugarcane Maturity Using High Spatial Resolution Remote Sensing Images. *Crops*, Vol. 4(3), 333–347. https://doi.org/10.3390/crops4030024.

[75] Som-ard, J., Atzberger, C., Izquierdo-Verdiguier, E., Vuolo, F. and Immitzer, M. (2021). Remote Sensing Applications in Sugarcane Cultivation: A Review. *Remote Sensing*, Vol. 13(20). https://doi.org/10.3390/rs13204040.

[76] Wang, C., Feng, M. C., Yang, W. D., Ding, G. W., Sun, H., Liang, Z. Y., Xie, Y. K. and Qiao, X. X., (2016). Impact of Spectral Saturation on Leaf Area Index and Aboveground Biomass Estimation of Winter Wheat. *Spectroscopy Letters*, Vol. 49(4), 241–248. https://doi.org/10.1080/00387010.2015.1133652.

[77] Chang, J. G., Kraatz, S., Anderson, M. and Gao, F., (2024). Enhanced Polarimetric Radar Vegetation Index and Integration with Optical Index for Biomass Estimation in Grazing Lands Across the Contiguous United States. *Remote Sensing*, Vol. 16(23). https://doi.org/10.3390/rs16234476.

[78] Garroutte, E., Hansen, A. and Lawrence, R., (2016). Using NDVI and EVI to Map Spatiotemporal Variation in the Biomass and Quality of Forage for Migratory Elk in the Greater Yellowstone Ecosystem. *Remote Sensing*, Vol. 8(5). https://doi.org/10.3390/rs8050404.

[79] Dou, H., Niu, G. and Gu, M., (2019). Photosynthesis, Morphology, Yield, and Phytochemical Accumulation in Basil Plants Influenced by Substituting Green Light for Partial Red and/or Blue Light. *HortScience*, Vol. 54(10), 1769–1776. https://doi.org/10.21273/HORTSCI14282-19.

[80] Rahman, M. M. and Robson, A., (2020). Integrating Landsat-8 and Sentinel-2 Time Series Data for Yield Prediction of Sugarcane Crops at the Block Level. *Remote Sensing*, Vol. 12(8). https://doi.org/10.3390/rs12081313.

[81] Rahman, M. M., Muir, J. and Robson, A. J., (2017). Multi-temporal Landsat Algorithms for the Yield Prediction of Sugarcane Crops in Australia. *7th Asian-Australasian Conference on Precision Agriculture*, October. https://doi.org/http://doi.org/10.5281/zenodo.891091.

[82] de Lima, I. P., Jorge, R. G. and de Lima, J. L. M. P., (2021). Remote Sensing Monitoring of Rice Fields: Towards Assessing Water Saving Irrigation Management Practices. *Frontiers in Remote Sensing*, Vol. 2, 1–13. https://doi.org/10.3389/frsen.2021.762093.

[83] Candiago, S., Remondino, F., De Giglio, M., Dubbini, M. and Gattelli, M. (2015). Evaluating Multispectral Images and Vegetation Indices for Precision Farming Applications from UAV Images. *Remote Sensing*, 7(4), 4026–4047. https://doi.org/10.3390/rs70404026.

[84] Pengphorm, P., Thongrom, S., Daengngam, C., Duangpan, S., Hussain, T. and Boonrat, P. (2024). Optimal-Band Analysis for Chlorophyll Quantification in Rice Leaves Using a Custom Hyperspectral Imaging System. *Plants*, Vol. 13(2). https://doi.org/10.3390/plants13020259.

[85] Ryu, J. H., Jeong, H. and Cho, J., (2020). Performances of Vegetation Indices on Paddy Rice at Elevated Air Temperature, Heat Stress, and Herbicide Damage. *Remote Sensing*, Vol. 12(16). https://doi.org/10.3390/rs12162654.

[86] Liu, J., Basnayake, J., Jackson, P. A., Chen, X., Zhao, J., Zhao, P., Yang, L., Bai, Y., Xia, H., Zan, F., Qin, W., Yang, K., Yao, L., Zhao, L., Zhu, J., Lakshmanan, P., Zhao, X. and Fan, Y., (2016). Growth and Yield of Sugarcane Genotypes are Strongly Correlated Across Irrigated and Rainfed Environments. *Field Crops Research*, Vol. 196, 418–425. https://doi.org/10.1016/j.fcr.2016.07.022.

[87] Rhyma, P. P., Norizah, K., Hamdan, O., Faridah-Hanum, I. and Zulfa, A. W., (2020). Integration of Normalised Different Vegetation Index and Soil-Adjusted Vegetation Index for Mangrove Vegetation Delineation. *Remote Sensing Applications: Society and Environment*, Vol. 17. https://doi.org/10.1016/j.rsase.2019.100280.

[88] Nagy, A., Szabó, A., Adeniyi, O. D. and Tamás, J., (2021). Wheat Yield Forecasting for the Tisza River Catchment Using Landsat 8 NDVI and SAVI Time Series and Reported Crop Statistics. *Agronomy*, Vol. 11(4). https://doi.org/ 10.3390/agronomy11040652.

[89] Pereira, R. M., Schwerz, F., Diotto, A. V., Oñate, C. A., Sandoval, M. D. V., Caron, B. O. and Cândido, B. (2025). Improving Water Use and Sugarcane Yield Using Irrigation Strategies in Nicaragua. *AgriEngineering*, Vol. 7(5). https://doi.org/10.3390/agriengineering7050162.